Inflammopharmacology (2022) 30:1369–1382
https://doi.org/10.1007/s10787-022-01021-y

Inflammopharmacology

ORIGINAL ARTICLE

Oxocrebanine from *Stephania pierrei* exerts macrophage anti-inflammatory effects by downregulating the NF-κB, MAPK, and PI3K/Akt signalling pathways

Wanatsanan Chulrik[1] · Chutima Jansakun[2] · Waraluck Chaichompoo[3] · Aman Tedasen[2] · Pathumwadee Yotmanee[4] · Apsorn Sattayakhom[2] · Wilanee Chunglok[5] · Apichart Suksamrarn[4] · Warangkana Chunglok[2,6]

Received: 26 April 2022 / Accepted: 13 June 2022 / Published online: 13 July 2022

Abstract

Plant-derived medicinal compounds are increasingly being used to treat acute and chronic inflammatory diseases, which are generally caused by aberrant inflammatory responses. *Stephania pierrei* Diels, also known as Sabu-lueat in Thai, is a traditional medicinal plant that is used as a remedy for several inflammatory disorders. Since aporphine alkaloids isolated from *S. pierrei* tubers exhibit diverse pharmacological characteristics, we aimed to determine the anti-inflammatory effects of crude extracts and alkaloids isolated from *S. pierrei* tubers against lipopolysaccharide (LPS)-activated RAW264.7 macrophages. Notably, the *n*-hexane extract strongly suppressed nitric oxide (NO) while exhibiting reduced cytotoxicity. Among the five alkaloids isolated from the *n*-hexane extract, the aporphine alkaloid oxocrebanine exerted considerable anti-inflammatory effects by inhibiting NO secretion. Oxocrebanine also significantly suppressed prostaglandin E_2, tumour necrosis factor-α, interleukin (IL)-1β, IL-6, inducible nitric oxide synthase, and cyclooxygenase (COX)-2 protein expression by inactivating the nuclear factor κB, c-Jun NH_2-terminal kinase, extracellular signal-regulated kinase 1/2, and phosphatidylinositol 3-kinase/Akt inflammatory signalling pathways. Molecular docking analysis further revealed that oxocrebanine has a higher affinity for toll-like receptor 4/myeloid differentiation primary response 88 signalling targets and the COX-2 protein than native ligands. Thus, our findings highlight the potential anti-inflammatory effects of oxocrebanine and suggest that certain alkaloids of *S. pierrei* could be used to treat inflammatory diseases.

Keyword Oxocrebanine · Aporphine alkaloid · *Stephania pierrei* · Inflammatory pathway · Cyclooxygenase

✉ Warangkana Chunglok
cwarang@wu.ac.th

1 Health Sciences (International Program), College of Graduate Studies, Walailak University, Nakhon Si Thammarat 80160, Thailand

2 School of Allied Health Sciences, Walailak University, Nakhon Si Thammarat 80160, Thailand

3 Department of Food and Pharmaceutical Chemistry, Faculty of Pharmaceutical Sciences, Chulalongkorn University, Bangkok 10330, Thailand

4 Department of Chemistry and Center of Excellence for Innovation in Chemistry, Faculty of Science, Ramkhamhaeng University, Bangkok 10240, Thailand

5 Division of Biological Science, Faculty of Science, Prince of Songkla University, Songkhla 90110, Thailand

6 Food Technology and Innovation Research Center of Excellence, Institute of Research and Innovation, Walailak University, Nakhon Si Thammarat 80160, Thailand

Introduction

Acute and chronic inflammatory diseases, including heart disease, stroke, pulmonary disease, respiratory infections, cancer, and diabetes mellitus, are among the top ten leading causes of death in the United States and worldwide (World Health Organisation 2020; Murphy et al. 2021). Steroids and nonsteroidal anti-inflammatory drugs (NSAIDs) with analgesic, antipyretic, and anti-inflammatory properties are among the most prescribed pharmaceuticals globally (Chhaya et al. 2016; Abdu et al. 2020); however, their numerous limitations and adverse effects (Giles et al. 2018; Wong 2019) have led to an increase in the use of plant-derived medicinal substances to treat inflammatory illnesses (Rezaieyazdi et al. 2019; Shi et al. 2021; Gandhi et al. 2021).

Macrophages are phagocytic, antigen-presenting, immunomodulatory cells that play critical roles in innate immune

system defences by secreting specific regulatory molecules (Wang et al. 2019). The transmembrane toll-like receptor 4 (TLR4) enables macrophages to recognize pathogens/lipopolysaccharide (LPS) and initiate intracellular signalling cascades through the classical myeloid differentiation primary response 88 (MyD88)-dependent and alternative MyD88-independent pathways (Ciesielska et al. 2021). The activation of the TLR4/MyD88 pathway regulates numerous cellular signalling pathways involving nuclear factor κB (NF-κB), mitogen-activated protein kinase (MAPK), and phosphatidylinositol 3-kinase (PI3K)/Akt, which induce inflammatory responses (Zhou et al. 2014). However, the excessive production of inflammatory mediators and cytokines by macrophages may damage host tissues and contribute towards the development of inflammatory diseases (Kany et al. 2019). To effectively treat inflammation, it is therefore necessary to develop powerful anti-inflammatory drugs that inhibit both the production and regulation of different inflammatory signalling molecules without generating adverse effects.

The genus *Stephania* (Menispermaceae) has long been used in traditional medicine to treat various ailments (Semwal et al. 2010). *Stephania pierrei* Diels, also known as Sabu-lueat in Thai (Intusaitrakul 2010), is a common traditional herb in South-East Asia (Dary et al. 2015) whose tubers are used as an ayurvedic herb, health tonic, analgesic, skeletal muscle relaxant, and treatment for diseases including cancer, diabetes, migraines, postpartum haemorrhage, leucorrhoea, and anaemia (Tantisewie and Ruchirawat 1992; Intusaitrakul 2010). Previous phytochemical studies have revealed that alkaloids are the major bioactive compounds in *S. pierrei* tubers (Maliwong et al. 2021; Chaichompoo et al. 2021) and that aporphine alkaloids isolated from *S. pierrei* can display anti-malarial (Likhitwitayawuid et al. 1993; Angerhofer et al. 1999) and anti-cholinesterase properties (Chaichompoo et al. 2021). Unfortunately, no research has been conducted on *S. pierrei* tubers and their immunomodulatory properties.

Aporphine alkaloids derived from *Stephania* have been reported to possess a variety of pharmacological activities, including anti-oxidant (Wang et al. 2020), anti-cancer (Yu et al. 2021), and anti-platelet (Jantan et al. 2006) effects. In addition, the aporphine alkaloids crebanine and dicentrine isolated from *S. venosa* tubers have been shown to suppress inflammatory mediators by inhibiting the inflammatory signalling molecules NF-κB, MAPK, Akt, and activator protein (AP)-1 in LPS-activated RAW264.7 macrophages (Intayoung et al. 2016; Yodkeeree et al. 2018). The aporphine alkaloid magnoflorine exhibited anti-inflammatory activity in LPS-activated human THP-1 macrophages by inactivating the MyD88/NF-κB pathway (Zhao et al. 2021). In terms of the response patterns to microbial ligands, surface markers, and functional characteristics, RAW264.7 and THP-1 macrophages closely mimic primary human macrophages and have been used to explore the immunomodulatory effects of various compounds or drugs (Berghaus et al. 2010; Chanput et al. 2014). Previously, we reported that (–)-stephanine and dehydrostephanine isolated from *S. venosa* tubers can reduce LPS-activated inflammatory cytokine production in murine macrophages (Chulrik et al. 2020). To establish whether *S. pierrei* tubers have immunomodulatory properties, we investigated the anti-inflammatory effects of crude extracts and compounds isolated from *S. pierrei* tubers in LPS-activated RAW264.7 and differentiated THP-1 macrophages. The molecular mechanism underlying the inhibition of inflammatory protein expression by a candidate aporphine alkaloid was performed using western blot analysis. Furthermore, we evaluated the modes of recognition and interaction between a candidate aporphine alkaloid and inflammatory protein targets by performing molecular docking analyses.

Materials and methods

Plant material extraction and isolation

S. pierrei tubers were collected from Prachin Buri Province, Thailand, in 2019. The plant species was identified by Assoc. Prof. Nopporn Dumrongsiri of Ramkhamhaeng University and a voucher specimen was deposited at the Faculty of Science, Ramkhamhaeng University (Apichart Suksamrarn, No. 101).

Extraction and isolation were carried out as described by Chaichompoo et al. (2021). Briefly, fresh *S. pierrei* tubers (1.5 kg) were extracted using *n*-hexane, EtOAc, and MeOH at 30 °C. Filtered solutions from each extraction were concentrated under reduced pressure at 40–45 °C to produce *n*-hexane (2.8 g), EtOAc (3.3 g), and MeOH (4.5 g) extracts, respectively. Since the *n*-hexane extract possessed the most potent anti-inflammatory effect (Fig. 1), it was selected for further chromatographic purification using a silica column (Merck KGaA, Darmstadt, Germany) eluted with a CH_2Cl_2–MeOH gradient to produce alkaloids at a sufficient quantity for biological evaluation: (–)-stephanine (433.0 mg, Fig. 2a), crebanine (240.0 mg, Fig. 2b), oxocrebanine (150.0 mg, Fig. 2c), dicentrine (68.0 mg, Fig. 2d), and stephapierrine B (50.6 mg, Fig. 2e). The structures of the isolated compounds were characterized using spectroscopic (IR, ^{1}H, ^{13}C NMR, and mass spectral) data and through comparison with previous literature (Chaichompoo et al. 2021).

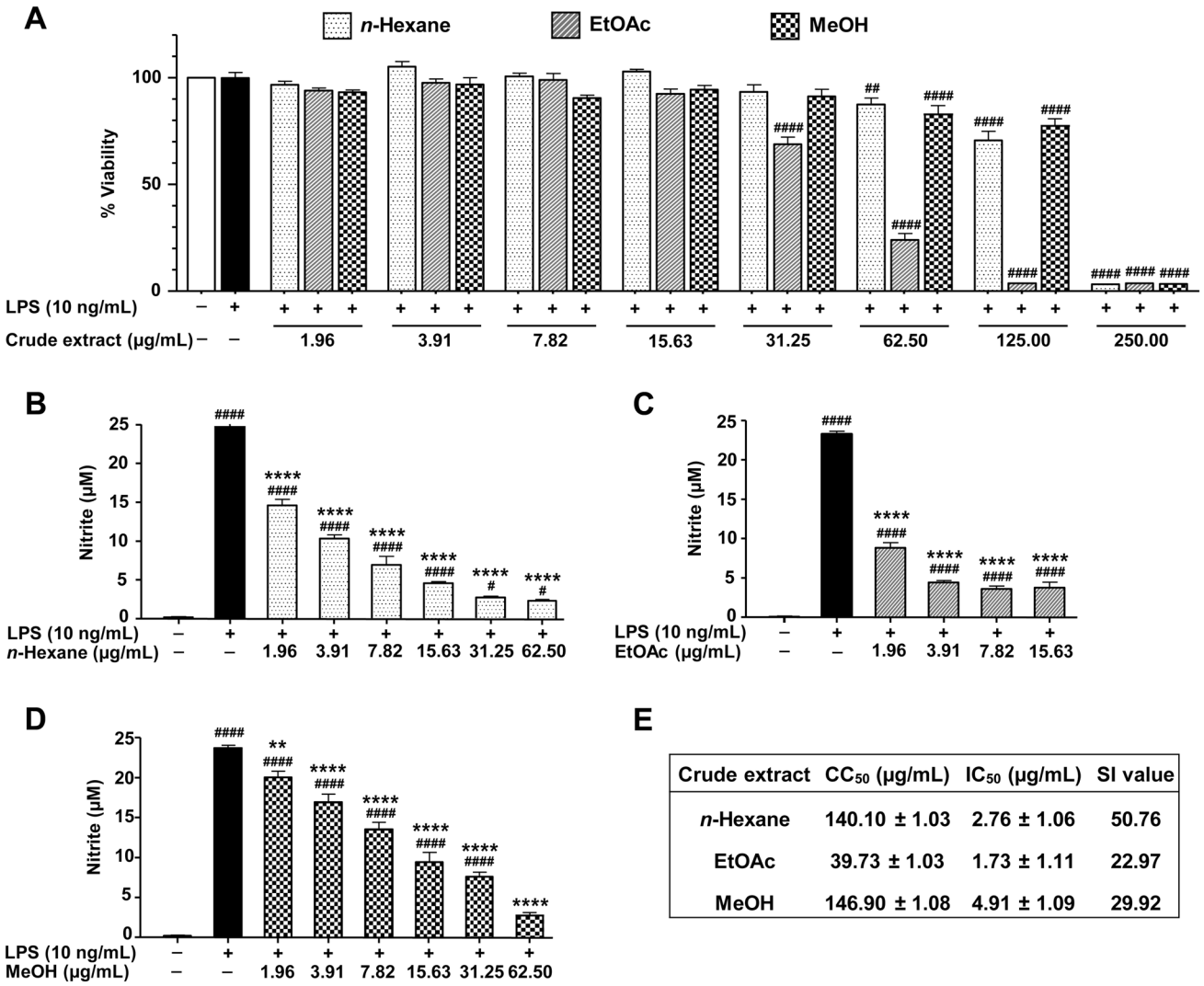

E

Crude extract	CC_{50} (μg/mL)	IC_{50} (μg/mL)	SI value
n-Hexane	140.10 ± 1.03	2.76 ± 1.06	50.76
EtOAc	39.73 ± 1.03	1.73 ± 1.11	22.97
MeOH	146.90 ± 1.08	4.91 ± 1.09	29.92

Fig. 1 Effects of *n*-hexane, EtOAc, and MeOH extracts from *S. pierrei* tubers on cell viability and NO production in LPS-activated RAW264.7 macrophages. **a** Viability of RAW264.7 macrophages treated with *n*-hexane, EtOAc, and MeOH extracts at various concentrations (1.96–250.00 μg/mL) determined using the MTT assay. NO inhibitory activity of non-toxic doses of **b** *n*-hexane, **c** EtOAc, and **d** MeOH extracts determined using the Griess assay. **e** Selectivity index (SI) values calculated for each crude extract using a ratio of the half-maximal cytotoxic concentration (CC_{50}) to the half-maximal NO inhibitory concentration (IC_{50}). "–" and "+" indicate the absence and presence of a compound, respectively. Values represent the mean ± SEM of three independent experiments performed in triplicate. #$p < 0.05$, ##$p < 0.01$, ####$p < 0.0001$ vs. untreated control; **$p < 0.01$, ****$p < 0.0001$ vs. LPS-stimulated cells

Cell culture

Murine RAW264.7 macrophages purchased from the American Type Culture Collection (ATCC; Manassas, VA, USA) and human monocyte cell line THP-1 obtained from the Cell Lines Service (CLS; Eppelheim, Baden-Württemberg, Germany) were grown in RPMI-1640 (Corning, New York, USA) supplemented with 10% endotoxin-free foetal bovine serum (Biochrom GmbH, Berlin, Germany), penicillin (100 U/mL), streptomycin (100 U/mL), and 2 mM L-glutamine (Gibco, Gaithersburg, MD, USA) in a humidified 5% CO_2 atmosphere at 37 °C. To induce THP-1 human monocytes differentiated into macrophages, cells were differentiated by 100 nM phorbol 12-myristate 13-acetate (PMA; Sigma-Aldrich, Saint Louis, MO, USA) for 48 h. Differentiated THP-1 cells were refreshed with RPMI-1640 without PMA for another 24 h and then incubated with oxocrebanine (10, 20, and 40 μM) for 1 h, followed by 10 ng/mL LPS for 24 h.

MTT assay

The cytotoxicity of crude extracts and alkaloids isolated from *S. pierrei* in LPS-activated RAW264.7 macrophages

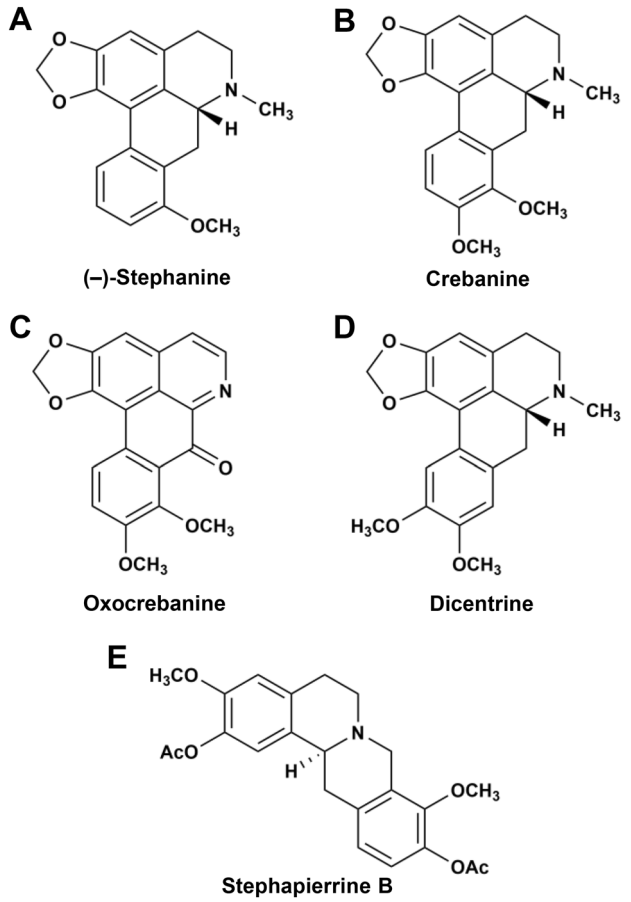

Fig. 2 Structures of **a** (–)-stephanine, **b** crebanine, **c** oxocrebanine, **d** dicentrine, and **e** stephapierrine B isolated from the *n*-hexane extract of *S. pierrei* tubers

was determined using 3-(4,5-dimethylthiazol-2-yl)-2,5-diphenyltetrazolium bromide (MTT; Sigma-Aldrich). Briefly, RAW264.7 macrophages (3.2×10^4 cells/cm^2) were seeded into 96-well plates, pre-treated with different alkaloid concentrations for 1 h, and treated with 10 ng/mL LPS from *Escherichia coli* 0111:B4 (Sigma-Aldrich) for 24 h. The cells were then incubated with 100 µL of MTT solution (0.5 mg/mL) for another 3 h at 37 °C. After the solution had been discarded, formazan crystals in each well were dissolved in 200 µL of dimethyl sulfoxide and the absorbance was detected at 560 nm using a microplate reader (Thermo Fisher, Waltham, MA, USA).

Griess assay

To monitor nitric oxide (NO) production, we detected nitrite, a stable end product of NO formation, using Griess reagent. Briefly, RAW264.7 macrophages (3.2×10^4 cells/cm^2) were seeded into 96-well plates, pre-treated with non-toxic doses of each compound for 1 h, and stimulated with LPS (10 ng/mL) for 24 h. The culture medium was collected and treated with Griess reagent, as described previously (Sun et al. 2003). The absorbance was measured at 540 nm using a microplate reader and nitrite levels were calculated based on the sodium nitrite standard curve with $r^2 > 0.999$.

Selectivity index (SI)

The SI of each extract and compound was calculated as the ratio of the half-maximal cytotoxic concentration (CC_{50}) and the half-maximal inhibitory concentration (IC_{50}) of NO from a dose–response curve using non-linear regression in GraphPad Prism version 9.3.0. (GraphPad Software, San Diego, CA, USA).

Enzyme-linked immunosorbent assay (ELISA)

RAW264.7 and differentiated THP-1 macrophages were seeded at a density of 3.2×10^4 cells/cm^2 into 96-well plates for 24 h, pre-treated with 10–40 µM oxocrebanine or 10 µM dexamethasone for 1 h, and stimulated with 10 ng/mL LPS for 24 h. The culture supernatants were then collected and the levels of inflammatory cytokines (tumour necrosis factor-α (TNF-α), interleukin (IL)-1β, and IL-6; BioLegends, San Diego, CA, USA) and prostaglandin E_2 (PGE_2; Abcam, Cambridge, UK) were determined according to the manufacturer's instructions.

Western blot analysis

To investigate the mechanism of oxocrebanine's anti-inflammation action, a western blot experiment was used to detect specific inflammatory proteins and measure relative protein expression. RAW264.7 macrophages were seeded at a density of 3.2×10^4 cells/cm^2 into 6-well plates for 24 h and pre-treated with 10–40 µM oxocrebanine, 10 µM dexamethasone, 25 µM LY 294002, or 5 µM BAY 11–7082 for 1 h. Next, the cells were stimulated with LPS (10 ng/mL) for 24 h to determine inducible nitric oxide synthase (iNOS) and cyclooxygenase (COX)-2 expression or for 30 min to detect the expression of NF-κB, MAPK, and PI3K/Akt. After the cells had been washed with ice-cold phosphate-buffered saline and incubated with lysis buffer containing protease inhibitors (Cell Signaling Technology, Danvers, MA, USA), the supernatant was collected by centrifugation at 16,000 rpm for 10 min at 4 °C, and the protein concentration was quantified using a bicinchoninic acid protein assay kit (Thermo Fisher). Protein samples (30–50 µg) were separated using sodium dodecyl sulfate–polyacrylamide gel electrophoresis and transferred onto polyvinylidene fluoride membranes (BioRad Laboratories, CA, USA). The membranes were blocked for 1 h with 5% non-fat milk at 25 °C and incubated at 4 °C overnight with primary antibodies against iNOS, COX-2, p-p65, p65, p-inhibitor of κB kinase

(IKK) α/β, IKKβ, p-inhibitor of κBα (IκBα), IκBα, p-stress-activated protein kinase (SAPK)/c-Jun N-terminal kinase (JNK), SAPK/JNK, p-extracellular-signal-regulated kinase (ERK) 1/2, ERK1/2, p-p38, p38, p-PI3K, PI3K, p-Akt, Akt, or β-actin (1:1,000; Cell Signaling Technology). After washing with Tris-buffered saline and 0.1% Tween 20, the membranes were incubated with anti-rabbit or anti-mouse HRP-conjugated secondary antibodies (1:2,000; Cell Signaling Technology). Protein bands were visualized using Luminata Forte ECL reagent (Merck KGaA) and detected using Image Lab™ Touch Software (BioRad Laboratories). Proteins were quantified using Image J software version 1.8.0 (National Institute of Health, Bethesda, MD, USA) and the ratio of target protein/β-actin or phosphorylated form/total form was calculated. A low relative density ratio indicates that oxocrebanine inhibits the expression of target inflammatory proteins, whereas a high ratio indicates the opposite.

In silico molecular docking analysis

To monitor the intermolecular interactions between oxocrebanine and target proteins, molecular docking analysis was performed using AutoDock (ATD) software version 4.2 (Morris et al. 1998). The three-dimensional (3D) crystal structures of 20 inflammation-related target proteins were obtained from the Research Collaboratory for Structural Bioinformatics (RCSB) Protein Data Bank (PDB) (www.rcsb.org) with a resolution of less than 3.5 angstroms (Å). The PDB codes corresponding to each protein are listed in Table 1. Ligands or inhibitors were removed from the protein structure before docking using the Visual Molecular Dynamic (VMD) package. After water molecules had been removed, all polar hydrogen atoms were added to the proteins using ATD software. The protein structures were saved as PDB, Partial Charge (Q), and Atom Type (T) or PDBQT format files.

For ligand preparation, the 3D-structures of oxocrebanine and reference ligands were obtained from the PubChem ligand structure database (www.pubchem.ncbi.nlm.nih.gov) and were written into the PDB files using the Online SMILES Translator and Structure File Generator (https://cactus.nci.nih.gov/translate/). All polar hydrogen molecules were added using ADT software and the structures were saved as PDBQT format files.

AutoDock Tools (Morris et al. 2009) were used to prepare grid maps for the semi-flexible docking protocol, where the protein molecule was kept rigid and the ligand flexible. Partial atomic charges of the proteins and ligands were assigned using the Gasteiger-Marsili method (Gasteiger and Marsili 1980). A cubical grid was individually created and centred on the region covering all the identified active pocket amino acid residues. ATD software was used with Lamarckian genetic algorithms and the default protocol for 50 docking runs with a population size of 200 for all docking analyses to seek the best binding site for oxocrebanine in the target proteins. The docked conformation with the lowest binding energy ($\Delta G_{docking}$; kcal/mol) and the corresponding inhibitory constant (K_i) in the most populated cluster was selected for each compound. Docking results were visualized using the Biovia Discovery Studio Visualizer (Dassault Systèmes BIOVIA, San Diego, CA, USA).

Table 1 The binding affinities of oxocrebanine and native ligands for the inflammatory protein targets

Protein	PDB ID	Oxocrebanine		Native ligand	
		$\Delta G_{docking}$ (Kcal/mol)	K_i (μM)	$\Delta G_{docking}$ (Kcal/mol)	K_i (μM)
MD2	2E59	−7.77	2.02	−7.37	3.98
TLR4	3FXI	−6.17	30.12	−4.54	470.78
MyD88	3MOP	−6.37	21.52	−5.11	180.38
IRAK1	6BFN	−8.29	0.84	−8.12	1.12
IRAK4	4Y73	−6.95	8.00	−7.69	2.31
TRAF6	1LB5	−6.17	30.16	−7.14	5.81
TAK1	4L3P	−7.88	1.69	−8.50	0.59
IKKβ	4KIK	−7.36	4.06	−5.89	19.09
IκBα	1NFI	−5.49	0.95	−5.11	0.18
p65 NF-κB	1NFI	−5.47	98.64	−4.14	916.61
MEK1	2P55	−7.35	3.91	−8.40	0.70
ERK1	2ZOQ	−6.97	7.79	−10.68	0.01
ERK2	6RQ4	−6.85	9.56	−7.59	2.71
JNK	3V6R	−7.33	4.25	−6.78	10.78
PI3K	3S2A	−7.63	2.54	−7.33	4.26
Akt2	2UW9	−5.99	1.95	−10.35	0.03
GSK3β	4ACG	−7.64	2.53	−6.53	16.47
iNOS	4NOS	−6.68	12.69	−7.51	3.14
COX-2	5F1A	−8.07	1.22	−7.57	2.85
TNF-α	2AZ5	−7.44	3.36	−8.17	1.02

PDB protein data bank, $\Delta G_{docking}$ lowest binding energy, K_i corresponding inhibitory constant, *MD2* myeloid differentiation factor 2, *TLR4* toll-like receptors 4, *MyD88* myeloid differentiation primary response 88, *IRAK*1 IL-1 receptor-associated kinase 1, *TRAF6* TNF receptor associated factor 6, *TAK1* transforming growth factor-β-activated kinase 1, *IKKβ* inhibitor of κB kinase β, *IκBα* inhibitor of κBα, *p65 NF-κB* p65 nuclear factor κB, *MEK1* mitogen-activated protein kinase kinase 1, *ERK* extracellular-signal-regulated kinase, *JNK* c-Jun N-terminal kinase, *PI3K* phosphatidylinositol 3-kinase, *GSK3β* glycogen synthase kinase 3β, *iNOS* inducible nitric oxide synthase, *COX-2* cyclooxygenase-2, *TNF-α* tumor necrosis factor-α

Statistical analysis

All experimental data were expressed as the mean ± standard error of the mean (SEM) of three independent experiments. Significant differences among the treatment groups ($p < 0.05$) were analysed using one-way analysis of variance followed by Dunnett's multiple comparison test in GraphPad

Prism version 9.3.0 (GraphPad Software, La Jolla, CA, USA).

Results

Effects of *n*-hexane, EtOAc, and MeOH extracts from *S. pierrei* on cell viability and NO inhibition

First, we examined the effects of crude *n*-hexane, EtOAc, and MeOH extracts isolated from *S. pierrei* tubers on cytotoxicity and NO production in LPS-induced RAW264.7 macrophages. Treatment with the *n*-hexane and MeOH extracts up to 62.50 µg/mL and EtOAc extract at 15.63 µg/mL yielded a cell viability of > 80% (Fig. 1a). Meanwhile, the *n*-hexane, EtOAc, and MeOH extracts significantly decreased NO levels in a dose-dependent manner, with IC_{50} values of 2.76 ± 1.06, 1.73 ± 1.11, and 4.91 ± 1.09 µg/mL, respectively (Figs. 1b–e). Among the three extracts, the *n*-hexane extract had the highest SI value (~ 51), which indicates selectivity for inhibiting NO secretion rather than general toxicity. Thus, the *n*-hexane extract appeared to be the most potent crude extract for NO inhibition (Fig. 1e).

Effects of alkaloids isolated from the *S. pierrei* n-hexane extract on cell viability and NO inhibition

Five alkaloids were obtained from the *n*-hexane extract of *S. pierrei* tubers in sufficient quantities for testing: (–)-stephanine, crebanine, oxocrebanine, dicentrine, and stephapierrine B (Fig. 2). In terms of cytotoxicity, the aporphine alkaloids (–)-stephanine, crebanine, oxocrebanine, and dicentrine and the tetrahydroprotoberberine alkaloid stephapierrine B had CC_{50} values of 51.20 ± 1.07, 70.57 ± 1.05, 90.60 ± 1.08, 19.28 ± 1.02 µM, and > 160 µM, respectively (Fig. 3a, g). Non-toxic doses of crebanine, oxocrebanine, and stephapierrine B dose-dependently decreased LPS-induced NO levels (Fig. 3c, d, f) with IC_{50} values of 5.68 ± 1.06, 3.37 ± 1.07, and 30.56 ± 1.14 µM, respectively (Fig. 3g). Notably, oxocrebanine was the most potent isolated alkaloid as it had the highest SI value (~ 27; Fig. 3g) besides the positive control drug dexamethasone (~ 38; Fig. 3g and Supplementary Fig. S1). Therefore, oxocrebanine was selected for further analysis of its potential anti-inflammatory molecular mechanisms.

Effect of oxocrebanine on the production of inflammatory mediators

Since oxocrebanine doses of 10–40 µM were non-toxic to RAW264.7 macrophages (Fig. 3a), we used these doses to investigate its effects on TNF-α, IL-1β, IL-6, and PGE_2 levels and the expression of iNOS and COX-2 in LPS-stimulated RAW264.7 cells. LPS stimulation markedly increased the secretion of TNF-α, IL-1β, IL-6, and PGE_2 and the protein expression of iNOS and COX-2 compared to the untreated control (Fig. 4); however, pre-treating the cells with oxocrebanine dose-dependently decreased TNF-α, IL-1β, IL-6, and PGE_2 secretion (Fig. 4a–d). Oxocrebanine at 40 µM significantly downregulated iNOS and COX-2 protein expression compared to the LPS-stimulated cells ($p < 0.01$ and $p < 0.001$, respectively) (Fig. 4e–f).

We also investigated the reduction in inflammatory cytokine levels following oxocrebanine treatment in LPS-activated differentiated THP-1 macrophages. Consistent with our findings in RAW264.7 macrophages, oxocrebanine treatment at 5–40 µM did not affect the viability of differentiated THP-1 cells (Fig. 5a). Furthermore, oxocrebanine (10–40 µM) dose-dependently inhibited IL-6 and TNF-α production in LPS-activated differentiated THP-1 macrophages (Fig. 5b, c). Together, these results indicate that oxocrebanine exerts anti-inflammatory effects by inhibiting various inflammatory cytokines and mediators in both RAW264.7 and differentiated THP-1 cells stimulated with LPS.

Effect of oxocrebanine on the NF-κB, MAPK, and PI3K/Akt signalling pathways

To elucidate the molecular mechanisms underlying the anti-inflammatory properties of oxocrebanine, which may be due to the suppression of inflammatory signalling pathways, we evaluated the effect of oxocrebanine on the NF-κB pathway using western blot analysis. Pre-treatment with 40 µM oxocrebanine significantly suppressed LPS-induced IKKα/β, IκBα, and p65 NF-κB protein phosphorylation in RAW264.7 macrophages compared to LPS-treated cells ($p < 0.05$, $p < 0.001$, and $p < 0.01$, respectively) (Fig. 6a). The IKKα/β inhibitor BAY 11–7082 (5 µM) markedly suppressed IKKα/β and IκBα phosphorylation.

Next, we investigated the expression of proteins related to the MAPK signalling pathways, including SAPK/JNK, ERK1/2, and p38. As shown in Fig. 6b, LPS stimulation significantly increased SAPK/JNK, ERK1/2, and p38 phosphorylation. Although treatment with 40 µM oxocrebanine significantly decreased the LPS-induced phosphorylation of SAPK/JNK and ERK1/2 ($p < 0.01$ and $p < 0.05$, respectively), neither oxocrebanine nor dexamethasone affected p38 phosphorylation.

In the PI3K/Akt pathway, LPS markedly increased PI3K and Akt phosphorylation. Meanwhile, oxocrebanine (40 µM) significantly suppressed PI3K protein phosphorylation ($p < 0.01$) and pre-treatment with 10–40 µM oxocrebanine dose-dependently decreased Akt phosphorylation ($p < 0.001$ and $p < 0.0001$) (Fig. 6c), similar to 25 µM LY 294002.

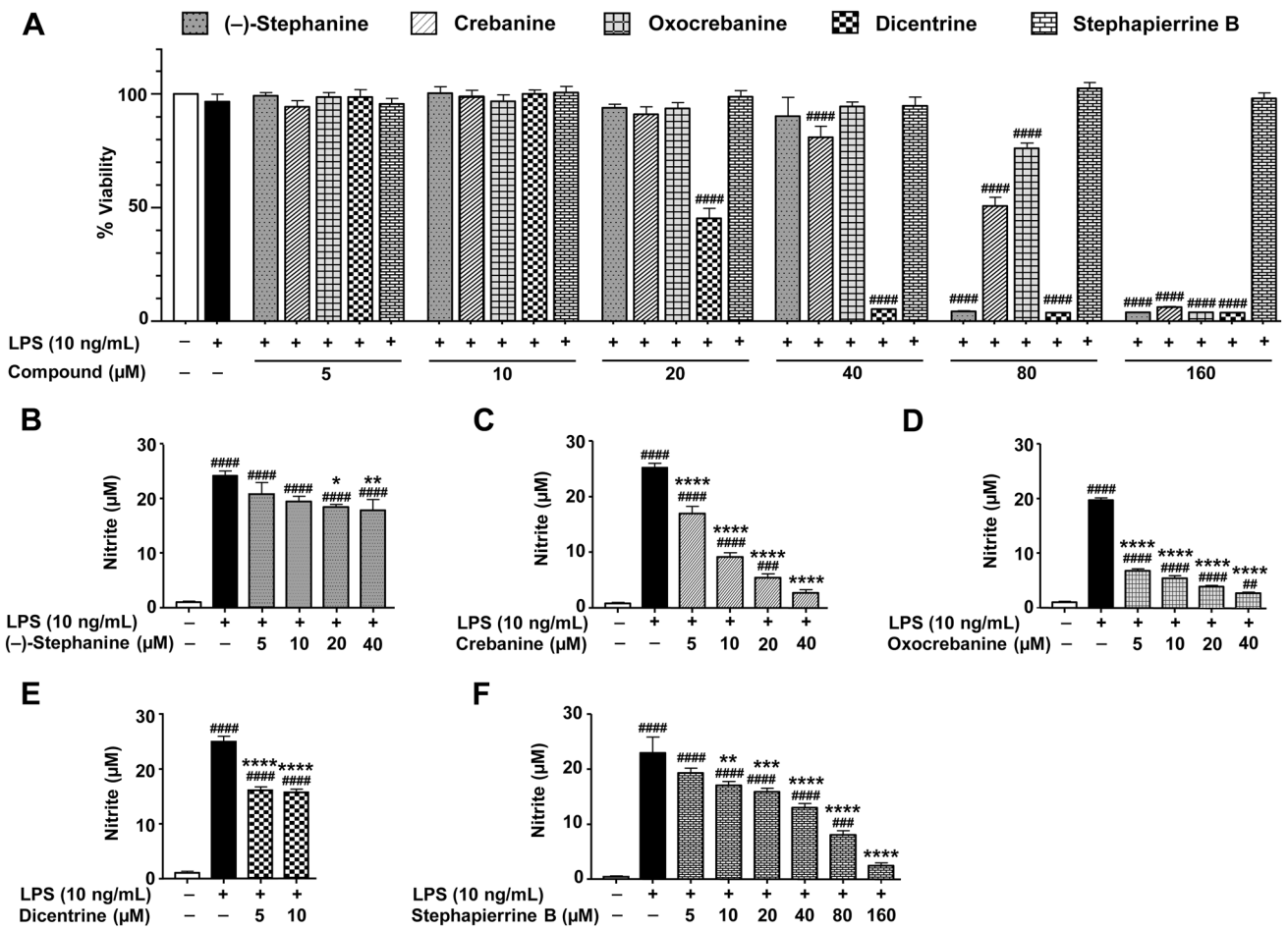

G

Compound	CC_{50} (μM)	IC_{50} (μM)	SI value
(–)-Stephanine	51.20 ± 1.07	> 40.00	> 1.28
Crebanine	70.57 ± 1.05	5.68 ± 1.06	12.42
Oxocrebanine	90.60 ± 1.08	3.37 ± 1.07	26.88
Dicentrine	19.28 ± 1.02	> 10.00	> 1.93
Stephapierrine B	> 160.00	30.56 ± 1.14	> 5.24
Dexamethasone	> 160.00	4.26 ± 1.09	> 37.56
BAY 11-7082	8.57 ± 1.03	1.24 ± 1.05	6.91
LY 294002	> 80.00	27.10 ± 1.08	> 2.95

Fig. 3 Effects of alkaloids isolated from the *n*-hexane extract of *S. pierrei* tubers, including (–)-stephanine, crebanine, oxocrebanine, dicentrine, and stephapierrine B on **a** cell viability and **b–f** NO production in LPS-activated RAW264.7 macrophages using MTT and Griess assays, respectively. **g** Selectivity index (SI) values calculated for each alkaloid using a ratio of the half-maximal cytotoxic concentration (CC_{50}) and the half-maximal NO inhibitory concentration (IC_{50}) after treatment. "–" and "+" indicate the absence and presence of a compound, respectively. Values represent the mean ± SEM of three independent experiments performed in triplicate. ##$p < 0.01$, ###$p < 0.001$, ####$p < 0.0001$ vs. untreated control; *$p < 0.05$, **$p < 0.01$, ***$p < 0.001$, ****$p < 0.0001$ vs. LPS-stimulated cells

Together, these data suggest that oxocrebanine affects the NF-κB, MAPK, and PI3K/Akt signalling pathways in activated murine macrophages.

Molecular docking analysis of oxocrebanine and inflammation-related proteins

To predict the possible interactions between oxocrebanine and 20 inflammation-related proteins involved in LPS activation via the TLR4/MyD88 pathway and its

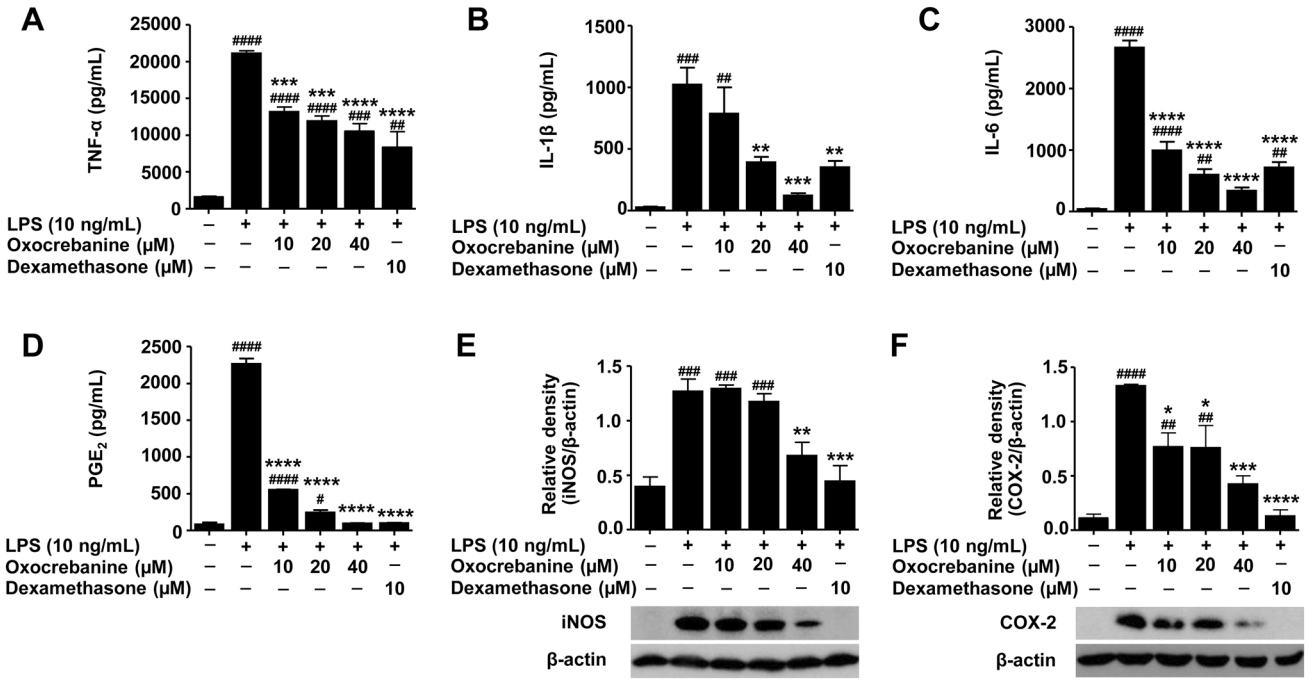

Fig. 4 Effect of oxocrebanine on the production of inflammatory mediators in LPS-activated RAW264.7 macrophages. **a** TNF-α, **b** IL-1β, **c** IL-6, and **d** PGE_2 levels were determined using ELISA. The expression of inflammatory proteins **e** iNOS and **f** COX-2 was determined using western blot analysis. "–" and "+" indicate the absence and presence of a compound, respectively. Values represent the mean ± SEM of three independent experiments. #$p < 0.05$, ##$p < 0.01$, ###$p < 0.001$, ####$p < 0.0001$ vs. untreated control; *$p < 0.05$, **$p < 0.01$, ***$p < 0.001$, ****$p < 0.0001$ vs. LPS-stimulated cells

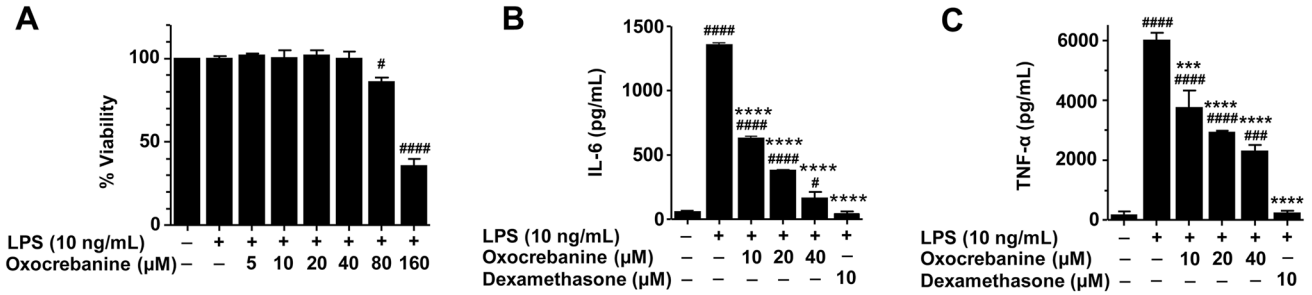

Fig. 5 Effect of oxocrebanine on cell viability and the production of inflammatory cytokines in LPS-activated differentiated THP-1 macrophages. **a** Cell viability determined by the MTT assay. **b** IL-6 and **c** TNF-α levels determined using ELISA. "–" and "+" indicate the absence and presence of the compounds, respectively. Values are expressed as the mean ± SEM of three independent experiments. #$p < 0.05$, ###$p < 0.001$, ####$p < 0.0001$ vs. untreated control; ***$p < 0.001$, ****$p < 0.0001$ vs. LPS-stimulated cells

downstream signalling components, we performed molecular docking analysis using ATD software. The binding energy and K_i values for oxocrebanine and native ligands with the inflammatory protein targets are summarized in Table 1. The potential protein targets of oxocrebanine were myeloid differentiation factor 2 (MD2; −7.77 kcal/mol, $K_i = 2.02$ μM), TLR4 (−6.17 kcal/mol, $K_i = 30.12$ μM), MyD88 (−6.37 kcal/mol, $K_i = 21.52$ μM), IL-1 receptor-associated kinase 1 (IRAK1; −8.29 kcal/mol, $K_i = 0.84$ μM), IKKβ (−7.36 kcal/mol, $K_i = 4.06$ μM), IκBα (−5.49 kcal/mol, $K_i = 0.95$ μM), p65 NF-κB (−5.47 kcal/mol, $K_i = 98.64$ μM), JNK (−7.33 kcal/mol, $K_i = 4.25$ μM), PI3K (−7.63 kcal/mol, $K_i = 2.54$ μM), glycogen synthase kinase 3β (GSK3β; −7.64 kcal/mol, $K_i = 2.53$ μM), and COX-2 (−8.07 kcal/mol, $K_i = 1.22$ μM), which had lower binding energy and K_i values than the native ligands (Fig. 7).

As shown in Table 2, oxocrebanine formed hydrogen bonds with the same amino acid residues as the native ligands, including TLR4 (TYR46 and LYS47), IRAK1 (LEU291), p65 NF-κB (ARG302 and THR305), JNK (MET149), and PI3K (VAL882). Moreover, identical hydrophobic patterns were observed for MD2 (ILE63), TLR4

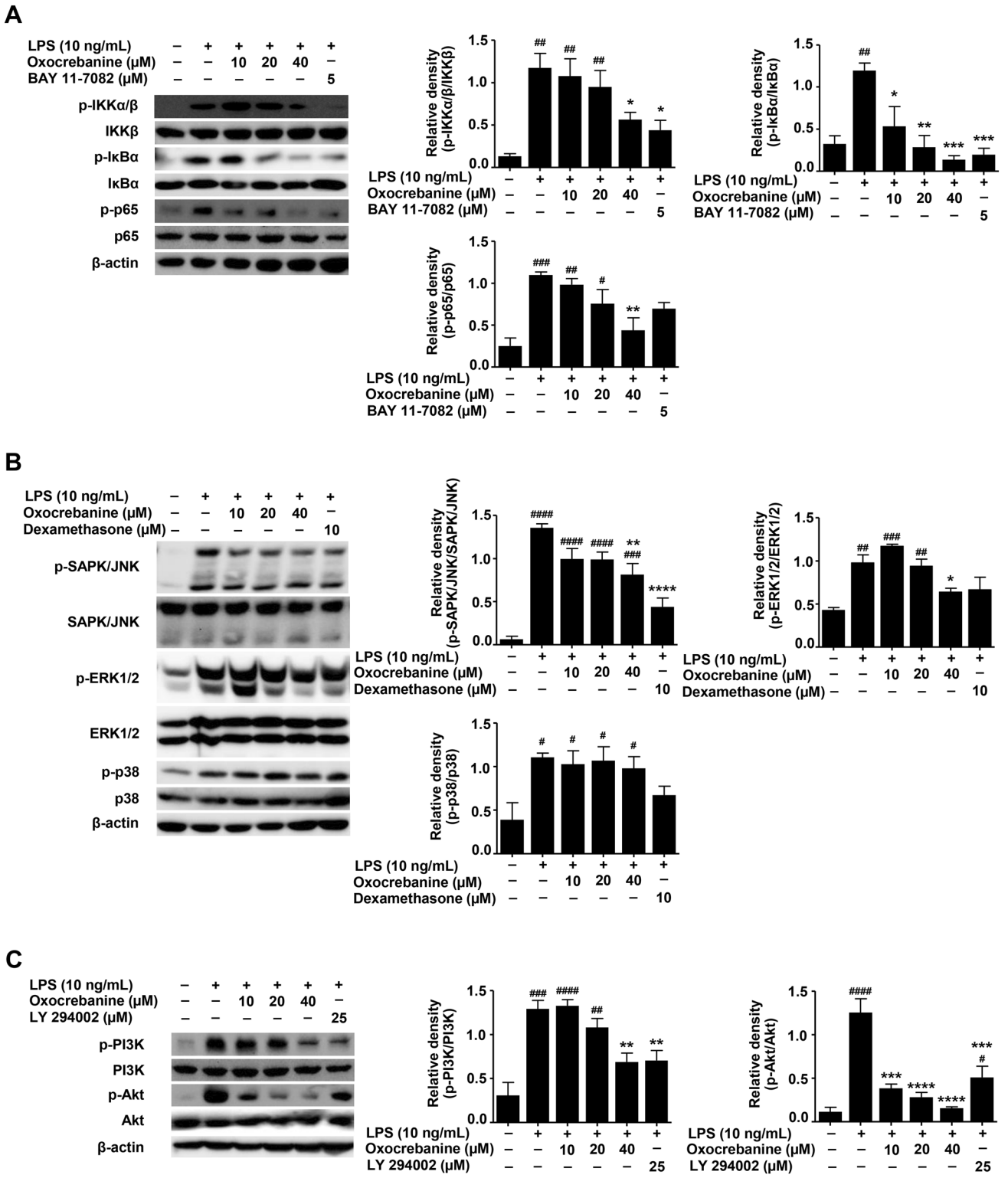

Fig. 6 Effect of oxocrebanine on NF-κB, MAPK, and PI3K/Akt signalling pathway activation in LPS-activated RAW264.7 macrophages. Western blot analysis and relative expression of phosphorylated forms normalized to total forms of **a** IKKα/β, IκBα, and p65 proteins **b** SAPK/JNK, ERK1/2, and p38 proteins, and **c** PI3K and Akt proteins. "–" and "+" indicate the absence and presence of a compound, respectively. Values represent the mean ± SEM of three independent experiments. #$p < 0.05$, ##$p < 0.01$, ###$p < 0.001$, ####$p < 0.0001$ vs. untreated control; *$p < 0.05$, **$p < 0.01$, ***$p < 0.001$, ****$p < 0.0001$ vs. LPS-stimulated cells

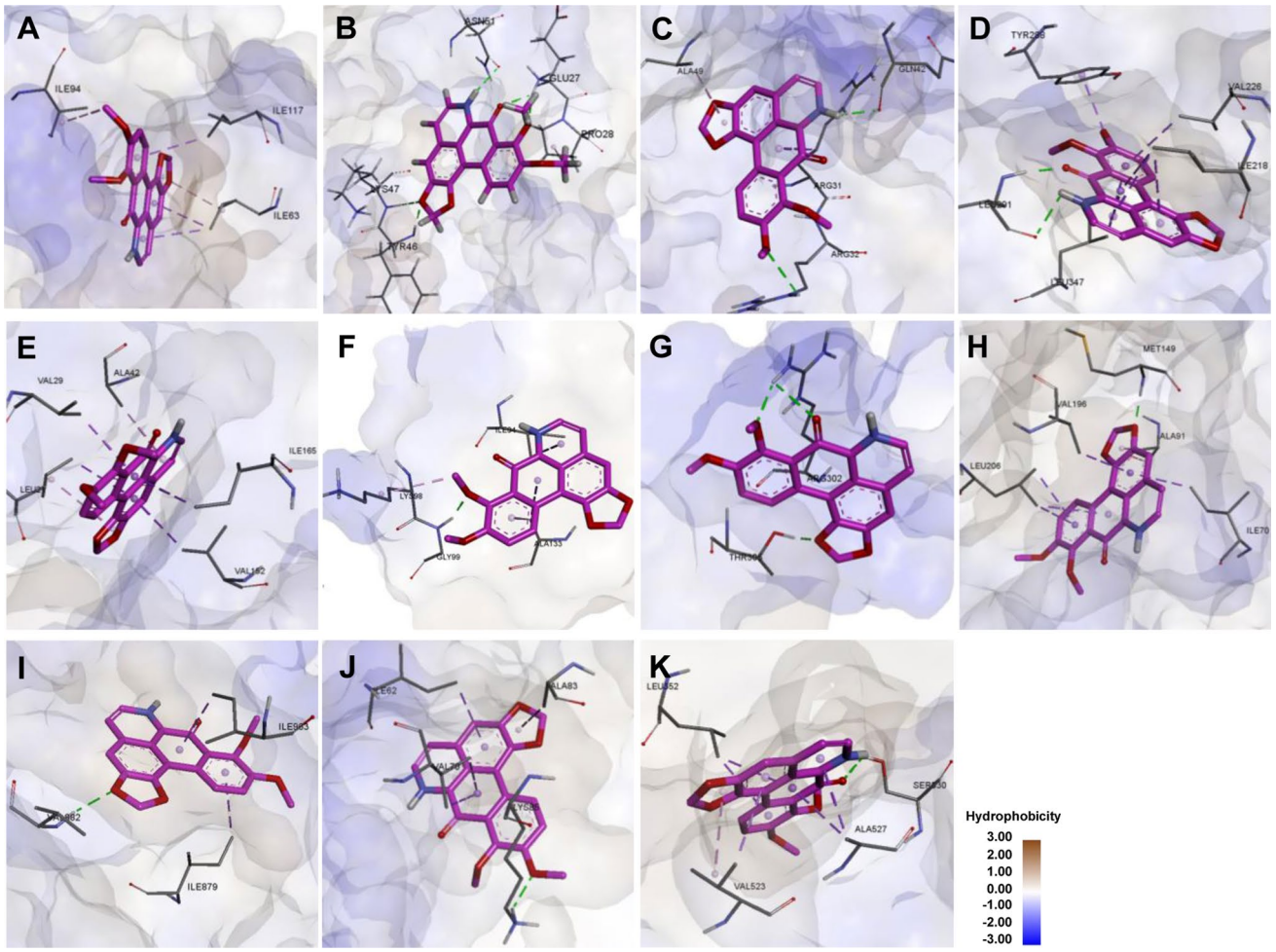

Fig. 7 3D images of the interactions between oxocrebanine (pink) and inflammatory protein targets determined using molecular docking analysis. Analysis of interactions between oxocrebanine and **a** MD2, **b** TLR4, **c** MyD88, **d** IRAK1, **e** IKKβ, **f** IκBα, (**g**) p65 NF-κB, **h** JNK, **i** PI3K, **j** GSK3β, and **k** COX-2. Pink, green, and purple dashed lines represent hydrophobic interactions, hydrogen bonding, and pi-sigma, respectively

(PRO28), IRAK1 (ILE218 and LEU347), IKKβ (LEU21, VAL29, and VAL152), IκBα (ILE94 and ALA133), JNK (VAL196), PI3K (ILE879), GSK3β (ILE62), and COX-2 (VAL523 and ALA527) when interacting with oxocrebanine and their native ligands (Supplementary Fig. S2 and Table S1). Taken together, these findings suggest that oxocrebanine exerts anti-inflammatory effects by interfering with multiple target inflammatory molecules.

Discussion

Natural products have gained increasing interest as immunomodulatory agents to treat inflammatory disorders due to the limitations and side effects of steroids and NSAIDs (Abdu et al. 2020; Giles et al. 2018). This study is the first to demonstrate that oxocrebanine, an aporphine alkaloid derived from *S. pierrei*, exhibits anti-inflammatory activity by inhibiting inflammatory mediators and cytokines in LPS-activated murine RAW264.7 and human differentiated THP-1 macrophages. Oxocrebanine might have the same anti-inflammatory effect on primary human macrophages as it does on LPS-activated THP-1 macrophages. THP-1 cells are human-based cell types with biological characteristics similar to that of human peripheral blood mononuclear cell-derived macrophages (Chanput et al. 2014). Furthermore, we found that these anti-inflammatory effects are mediated by oxocrebanine suppressing the NF-κB, MAPK, and PI3K/Akt signalling pathways and interfering with the binding of various inflammation-related proteins in the TLR4/MyD88 signalling pathways and COX-2.

NO is a critical inflammatory mediator that reflects the degree of inflammation and is overproduced in LPS-stimulated RAW264.7 macrophages (Isaksson et al. 2020). Among the five compounds isolated from *S. pierrei*, oxocrebanine was the best candidate compound for suppressing

Table 2 The binding interactions between amino acid residue of the potential proteins and oxocrebanine with the interaction distances

Protein	Interaction	Residue	Distance (Å)	Same amino acid residue with native ligand
MD2	Hydrophobic	ILE63, ILE117, ILE94	3.77/3.57/3.95, 3.98, 3.78	ILE63
TLR4	Hydrogen bond	GLU27, TYR46, LYS47, ASN51	2.11/2.87, 1.98, 2.81, 2.81	TYR46, LYS47
	Hydrophobic	PRO28	3.95	PRO28
MyD88	Hydrogen bond	ARG32, GLN42	2.74, 2.04	–
	Hydrophobic	ARG31, ALA49	3.74, 3.98	–
IRAK1	Hydrogen bond	LEU291	1.92/2.28	LEU291
	Hydrophobic	ILE218, VAL226, LEU347, TYR288	3.54/3.83/3.89, 3.80, 3.61/3.52, 3.56	ILE218, LEU347
IKKβ	Hydrophobic	LEU21, VAL29, VAL152, ILE165, ALA42	3.94/3.98, 3.95, 3.72, 3.97, 3.95	LEU21, VAL29, VAL152
IκBα	Hydrogen bond	GLY99	1.91	–
	Hydrophobic	ILE94, ALA133, LYS98	3.59, 3.80/3.93, 3.92	ILE94, ALA133
p65 NF-κB	Hydrogen bond	ARG302, THR305	2.60/2.12, 1.86	ARG302, THR305
JNK	Hydrogen bond	MET149	1.74	MET149
	Hydrophobic	ILE70, VAL196, LEU206, ALA91	3.87, 3.70, 3.88/3.45/3.78, 3.70	VAL196
PI3K	Hydrogen bond	VAL882	2.25	VAL882
	Hydrophobic	ILE879, ILE963	3.92, 3.86	ILE879
GSK3β	Hydrogen bond	LYS85	2.15	–
	Hydrophobic	ILE62, VAL70, ALA83	3.89, 3.67/3.89, 3.99	ILE62
COX-2	Hydrogen bond	SER530	2.21	–
	Hydrophobic	LEU352, VAL523, ALA527	3.73/3.53, 3.80/3.48, 3.56/3.46	VAL523, ALA527

Å angstrom, *MD2* myeloid differentiation factor 2, *TLR4* toll-like receptors 4, *MyD88* myeloid differentiation primary response 88, *IRAK1* IL-1 receptor-associated kinase 1, *IKKβ* inhibitor of κB kinase β, *IκBα* inhibitor of κBα, *p65 NF-κB* p65 nuclear factor κB, *JNK* c-Jun N-terminal kinase, *PI3K* phosphatidylinositol 3-kinase, *GSK3β* glycogen synthase kinase 3β, *COX-2* cyclooxygenase-2

NO secretion. Preliminary structure–activity experiments implied that the presence of a carbonyl group at the 7 position and the absence of the 6-N-methyl group in oxocrebanine may enhance its anti-inflammatory activity, as oxocrebanine is more effective at inhibiting NO production than crebanine. It has previously been reported that the presence of a 9-methoxy group on ring D of crebanine is required to suppress NO release and minimize cytotoxicity in LPS-induced BV2 cells, whereas ring D of (–)-stephanine lacks a 9-methoxy group (Xiao et al. 2021). In addition, the presence of a dimethoxy group at the C-9 and C-10 positions of dicentrine can increase its cytotoxicity (Yodkeeree et al. 2018). Our findings are consistent with previous reports that natural aporphine alkaloids isolated from the tubers of *Stephania* species (i.e., (–)-stephanine, crebanine, dicentrine, and dehydrostephanine) display anti-inflammatory activities in LPS-induced RAW264.7 macrophages by suppressing inflammatory mediators, NO, PGE_2, and cytokines (Intayoung et al. 2016; Yodkeeree et al. 2018; Chulrik et al. 2020).

In response to LPS-induced TLR4 signalling, the LPS/TLR4/MD2 complex on the cell surface of macrophages activates the classical MyD88-dependent pathway (Ciesielska et al. 2021). MyD88 activation leads to the recruitment and activation of downstream signals including IRAKs, TNF receptor-associated factor 6 (TRAF 6), and transforming growth factor-β-activated kinase 1 (TAK1) (Balan et al. 2019; Li et al. 2019). TAK1 subsequently phosphorylates and activates inflammatory signalling pathways such as the NF-κB, MAPK, and PI3K/Akt pathways to produce inflammatory mediators and cytokines (Endale et al. 2013; Haque et al. 2020). Previous studies have demonstrated that NF-κB signalling is a key target of aporphine alkaloids in various in vivo mouse models of inflammation (Pandurangan et al. 2016; Chen et al. 2018) and in vitro models of LPS-activated murine macrophages (Intayoung et al. 2016; Yodkeeree et al. 2018). Crebanine and *O*-methylbulbocapnine have also been shown to suppress the phosphorylation of p65 NF-κB, MAPK, and PI3K/Akt signalling proteins (Intayoung et al. 2016; Yodkeeree et al. 2018). Oxocrebanine, like dexamethasone (Jeon et al. 2000) and dicentrine (Yodkeeree et al. 2018), may have anti-inflammatory actions that are independent of p38 MAPK. Therefore, the anti-inflammatory effects of oxocrebanine in LPS-activated RAW264.7 macrophages appear to be achieved by inhibiting the NF-κB, MAPK, and PI3K/Akt signalling pathways.

Molecular docking analysis has been carried out to identify the mode of interaction between oxocrebanine and the active site of inflammatory proteins in the TLR4/MyD88 signalling pathways (da Silva et al. 2018). Notably, oxocrebanine was found to have multiple target inflammatory proteins in the TLR4/MyD88 signalling pathway and its

downstream signalling cascades. In this study, we found that oxocrebanine has a stronger binding energy than celecoxib for 5F1A-dependent COX-2 inhibition by forming hydrogen bonds with amino acid residue SER530 and interacting with LEU352, VAL523, and ALA527 via hydrophobic bonds. Consistently, selective COX-2 inhibitors have been shown to preferentially target amino acid residues SER530 and ALA527 in 5F1A (Bommu et al. 2019), among which SER530 plays an important role in the catalytic site of COX-2 and is the target of aspirin (Meade et al. 1993; Blobaum and Marnett 2007). Oxocrebanine may therefore function as a COX-2 inhibitor due to its interaction with certain key amino acid residues, consistent with the decreased COX-2 expression and PGE_2 levels observed in our cell model. Previous studies have demonstrated that aporphine alkaloids are effective inhibitors of COX-2 and 5-lipoxygenase (Barrera and Suárez 2010). Our docking analysis and biological experiments further suggest that oxocrebanine exerts anti-inflammatory effects by interfering with multiple target molecules in TLR4/MyD88 and COX-2 pathways.

Conclusion

The aporphine alkaloid oxocrebanine was isolated from *S. pierrei* and was found to alleviate inflammation by inhibiting NF-κB, MAPK, and PI3K/Akt signalling pathway activation in LPS-activated murine macrophages. In silico analyses further revealed that oxocrebanine interacts favourably with various protein targets associated with the TLR4/MyD88 signalling pathway, as evidenced by a strong binding affinity and the presence of key amino acid residues identical to native ligands. Together, the findings of this study suggest that oxocrebanine may be a promising agent for treating inflammatory disorders as it interferes with COX-2 binding and suppresses the COX-2/PGE_2 pathway. Because this research was only conducted in vitro, animal models of acute and chronic inflammatory diseases will be used to investigate the anti-inflammatory properties and therapeutic efficacy of oxocrebanine in vivo. Additional research is also needed to confirm its specific molecular targets, bioavailability, and safety for potential use in medicine.

Supplementary Information The online version contains supplementary material available at https://doi.org/10.1007/s10787-022-01021-y.

Acknowledgements This research was supported by the Thailand Science Research and Innovation Fund (Contract No. WU-FF64102) and the new strategic research (P2P) project of Walailak University, Nakhon Si Thammarat, Thailand (grant no. CGS-P2P-2564-054). W. Chulrik expresses her gratitude to the Walailak University Graduate Research Fund (grant no. CGS-RF-2021/05) and a Walailak University Ph.D. Excellence Scholarship (grant no. 04/2020). A. Suksamrarn and W. Chaichompoo acknowledge partial support from the Center of Excellence for Innovation in Chemistry, Ministry of Higher Education, Science, Research, and Innovation. We would like to thank Editage (www.editage.com) for English language editing.

Author contributions Conceptualization: WanC and WaranC; methodology: WanC, WaranC, and CJ; validation: WilC; formal analysis: AT and WaranC; investigation: WanC and WaralC; resources: ApsS and PY; writing—original draft preparation; WanC; writing—review and editing: WanC, WaranC and ApiS; supervision and funding acquisition: WaranC and ApiS. All authors read and approved the final manuscript.

Funding This research was supported by the Thailand Science Research and Innovation Fund (contract no. WU-FF64102) and the new strategic research (P2P) project of Walailak University, Nakhon Si Thammarat, Thailand (grant no. CGS-P2P-2564–054). W. Chulrik expresses her gratitude to the Walailak University Graduate Research Fund (grant no. CGS-RF-2021/05) and a Walailak University Ph.D. Excellence Scholarship (grant no. 04/2020).

Data availability All data presented in this study are included in the article.

Declarations

Conflict of interest The authors have no relevant financial or non-financial interests to disclose.

References

Abdu N, Mosazghi A, Teweldemedhin S et al (2020) Non-steroidal anti-inflammatory drugs (NSAIDs): Usage and co-prescription with other potentially interacting drugs in elderly: A cross-sectional study. PLoS ONE 15:e0238868. https://doi.org/10.1371/journal.pone.0238868

Angerhofer CK, Guinaudeau H, Wongpanich V, Pezzuto JM, Cordell GA (1999) Antiplasmodial and cytotoxic activity of natural bisbenzylisoquinoline alkaloids. J Nat Prod 62:59–66. https://doi.org/10.1021/np980144f

Balan I, Beattie MC, O'Buckley TK, Aurelian L, Morrow AL (2019) Endogenous neurosteroid (3α,5α)3-hydroxypregnan-20-one inhibits toll-like-4 receptor activation and pro-inflammatory signaling in macrophages and brain. Sci Rep 9:1220. https://doi.org/10.1038/s41598-018-37409-6

Barrera EDC, Suárez LEC (2010) *In vitro* inhibitory activities of Lauraceae aporphine alkaloids. Nat Prod Commun 5:383–386. https://doi.org/10.1177/1934578X1000500308

Berghaus LJ, Moore JN, Hurley DJ et al (2010) Innate immune responses of primary murine macrophage-lineage cells and RAW 264.7 cells to ligands of Toll-like receptors 2, 3, and 4. Comp Immunol Microbiol Infect 33:443–454. https://doi.org/10.1016/j.cimid.2009.07.001

Blobaum AL, Marnett LJ (2007) Structural and functional basis of cyclooxygenase inhibition. J Med Chem 50:1425–1441. https://doi.org/10.1021/jm0613166

Bommu UD, Konidala KK, Pamanji R, Yeguvapalli S (2019) Structural probing, screening and structure-based drug repositioning insights into the identification of potential Cox-2 inhibitors from selective coxibs. Interdiscip Sci 11:153–169. https://doi.org/10.1007/s12539-017-0244-5

Chaichompoo W, Rojsitthisak P, Pabuprapap W et al (2021) Stephapierrines A-H, new tetrahydroprotoberberine and aporphine alkaloids from the tubers of *Stephania pierrei* Diels and their

anti-cholinesterase activities. RSC Adv 11:21153–21169. https://doi.org/10.1039/d1ra03276c
Chanput W, Mes JJ, Wichers HJ (2014) THP-1 cell line: An *in vitro* cell model for immune modulation approach. Int Immunopharmacol 23:37–45. https://doi.org/10.1016/j.intimp.2014.08.002
Chen X, Zheng X, Zhang M, Yin H, Jiang K, Wu H (2018) Nuciferine alleviates LPS-induced mastitis in mice via suppressing the TLR4-NF-κB signaling pathway. Inflamm Res 67:903–911. https://doi.org/10.1007/s00011-018-1183-2
Chhaya V, Saxena S, Cecil E et al (2016) Steroid dependency and trends in prescribing for inflammatory bowel disease – a 20-year national population-based study. Aliment Pharm Ther 44:482–494. https://doi.org/10.1111/apt.13700
Chulrik W, Jansakun C, Chaichompoo W et al (2020) Dehydrostephanine isolated from *Stephania venosa* possesses anti-inflammatory activity in lipopolysaccharide-activated RAW264.7 macrophages. Walailak J Sci & Tech 17:655–664
Ciesielska A, Matyjek M, Kwiatkowska K (2021) TLR4 and CD14 trafficking and its influence on LPS-induced pro-inflammatory signaling. Cell Mol Life Sci 78:1233–1261. https://doi.org/10.1007/s00018-020-03656-y
da Silva DP, Florentino IF, da Silva DM et al (2018) Molecular docking and pharmacological/toxicological assessment of a new compound designed from celecoxib and paracetamol by molecular hybridization. Inflammopharmacology 26:1189–1206. https://doi.org/10.1007/s10787-018-0516-7
Dary C, Hul S, Kim S, Jabbour F (2015) Lectotypification of *Stephania pierrei* (Menispermaceae). Edinb J Bot 72:423–428. https://doi.org/10.1017/S0960428615000177
Endale M, Park SC, Kim S et al (2013) Quercetin disrupts tyrosine-phosphorylated phosphatidylinositol 3-kinase and myeloid differentiation factor-88 association, and inhibits MAPK/AP-1 and IKK/NF-κB-induced inflammatory mediators production in RAW 264.7 cells. Immunobiology 218:1452–1467. https://doi.org/10.1016/j.imbio.2013.04.019
Gandhi GR, Jothi G, Mohana T et al (2021) Anti-inflammatory natural products as potential therapeutic agents of rheumatoid arthritis: A systematic review. Phytomedicine 93:153766. https://doi.org/10.1016/j.phymed.2021.153766
Gasteiger J, Marsili M (1980) Iterative partial equalization of orbital electronegativity—A rapid access to atomic charges. Tetrahedron 36:3219–3228
Giles AJ, Hutchinson MKN, Sonnemann HM et al (2018) Dexamethasone-induced immunosuppression: Mechanisms and implications for immunotherapy. J Immunother Cancer 6:1–13. https://doi.org/10.1186/s40425-018-0371-5
Haque MA, Jantan I, Harikrishnan H, Ahmad W (2020) Standardized ethanol extract of *Tinospora crispa* upregulates pro-inflammatory mediators release in LPS-primed U937 human macrophages through stimulation of MAPK, NF-κB and PI3K-Akt signaling networks. BMC Complement Med Ther 20:245. https://doi.org/10.1186/s12906-020-03039-7
Intayoung P, Limtrakul P, Yodkeeree S (2016) Antiinflammatory activities of crebanine by inhibition of NF-κB and AP-1 activation through suppressing MAPKs and Akt signaling in LPS-induced RAW 264.7 macrophages. Biol Pharm Bull 39:54–61. https://doi.org/10.1248/bpb.b15-00479
Intusaitrakul C (2010) Trakul Wan Thai, Volume 2. In: Intusaitrakul C (ed) *Stephania pierrei* Diels. Duangkamol Publishing, Bangkok, pp 272–274
Isaksson R, Casselbrant A, Elebring E, Hallberg M, Larhed M, Fändriks L (2020) Direct stimulation of angiotensin II type 2 receptor reduces nitric oxide production in lipopolysaccharide treated mouse macrophages. Eur J Pharmacol 868:172855. https://doi.org/10.1016/j.ejphar.2019.172855
Jantan I, Raweh SM, Yasin YHM, Murad S (2006) Antiplatelet activity of aporphine and phenanthrenoid alkaloids from *Aromadendron elegans* Blume. Phytother Res 20:493–496. https://doi.org/10.1002/ptr.1885
Jeon YJ, Han SH, Lee YW, Lee M, Yang KH, Kim HM (2000) Dexamethasone inhibits IL-1 beta gene expression in LPS-stimulated RAW 264.7 cells by blocking NF-kappa B/Rel and AP-1 activation. Immunopharmacology 48:173–183. https://doi.org/10.1016/s0162-3109(00)00199-5
Kany S, Vollrath JT, Relja B (2019) Cytokines in inflammatory disease. Int J Mol Sci 20:6008. https://doi.org/10.3390/ijms20236008
Li T, Li F, Liu X, Liu J, Li D (2019) Synergistic anti-inflammatory effects of quercetin and catechin via inhibiting activation of TLR4–MyD88-mediated NF-κB and MAPK signaling pathways. Phytother Res 33:756–767. https://doi.org/10.1002/ptr.6268
Likhitwitayawuid K, Angerhofer CK, Chai H, Pezzuto JM, Cordell GA, Ruangrungsi N (1993) Cytotoxic and antimalarial alkaloids from the tubers of *Stephania pierrei*. J Nat Prod 56:1468–1478. https://doi.org/10.1021/np50099a005
Maliwong J, Sahakitpichan P, Chimnoi N, Ruchirawat S, Kanchanapoom T (2021) Isoquinoline alkaloids from the tubers of *Stephania pierrei*. Phytochem Lett 43:140–144. https://doi.org/10.1016/j.phytol.2021.04.005
Meade EA, Smith WL, Dewitt DL (1993) Differential inhibition of prostaglandin endoperoxide synthase (cyclooxygenase) isozymes by aspirin and other non-steroidal anti-inflammatory drugs. J Biol Chem 268:6610–6614. https://doi.org/10.1016/S0021-9258(18)53294-4
Morris GM, Goodsell DS, Halliday RS et al (1998) Automated docking using a Lamarckian genetic algorithm and empirical binding free energy function. J Comput Chem 19:1639–1662
Morris GM, Huey R, Lindstrom W et al (2009) AutoDock4 and AutoDockTools4: Automated docking with selective receptor flexibility. J Comput Chem 30:2785–2791. https://doi.org/10.1002/jcc.21256
Murphy SL, Kochanek KD, Xu J, Arias E (2021) Mortality in the United States, 2020. NCHS Data Brief 427. https://doi.org/10.15620/cdc:112079
Pandurangan AK, Mohebali N, Hasanpourghadi M, Looi CY, Mustafa MR, Mohd Esa N (2016) Boldine suppresses dextran sulfate sodium-induced mouse experimental colitis: NF-κB and IL-6/STAT3 as potential targets. BioFactors 42:247–258. https://doi.org/10.1002/biof.1267
Rezaieyazdi Z, Farooqi A, Soleymani-Salehabadi H et al (2019) International multicenter randomized, placebo-controlled phase III clinical trial of β-D-mannuronic acid in rheumatoid arthritis patients. Inflammopharmacology 27:911–921. https://doi.org/10.1007/s10787-018-00557-2
Semwal DK, Badoni R, Semwal R, Kothiyal SK, Singh GJP, Rawat U (2010) The genus *Stephania* (Menispermaceae): Chemical and pharmacological perspectives. J Ethnopharmacol 132:369–383. https://doi.org/10.1016/j.jep.2010.08.047
Shi J, Weng JH, Mitchison TJ (2021) Immunomodulatory drug discovery from herbal medicines: Insights from organ-specific activity and xenobiotic defenses. Elife 10:e73673. https://doi.org/10.7554/eLife.73673
Sun J, Zhang X, Broderick M, Fein H (2003) Measurement of nitric oxide production in biological systems by using Griess reaction assay. Sensors 3:276–284. https://doi.org/10.3390/s30800276
Tantisewie B, Ruchirawat S (1992) Alkaloids from the plants of Thailand. In: Brossi A (ed) The Alkaloids: chemistry and Pharmacology, vol 41. Academic Press, Massachusetts, pp 1–40
Wang S, Liu R, Yu Q, Dong L, Bi Y, Liu G (2019) Metabolic reprogramming of macrophages during infections and cancer. Cancer Lett 452:14–22. https://doi.org/10.1016/j.canlet.2019.03.015

Wang R, Zhou J, Shi G, Liu Y, Yu D (2020) Aporphine and phenanthrene alkaloids with antioxidant activity from the roots of *Stephania tetrandra*. Fitoterapia 143:104551. https://doi.org/10.1016/j.fitote.2020.104551

Wong RSY (2019) Role of nonsteroidal anti-inflammatory drugs (NSAIDs) in cancer prevention and cancer promotion. Adv Pharmacol Sci 2019. https://doi.org/10.1155/2019/3418975

World Health Organisation (2020) The top 10 causes of death. World Health Organisation. https://www.who.int/news-room/fact-sheets/detail/the-top-10-causes-of-death. Accessed 20 February 2022

Xiao J, Wang Y, Yang Y, Liu J, Chen G, Lin B (2021) Natural potential neuroinflammatory inhibitors from *Stephania epigaea* HS Lo. Bioorg Chem 107:104597. https://doi.org/10.1016/j.bioorg.2020.104597

Yodkeeree S, Ooppachai C, Pompimon W, Limtrakul P (2018) *O*-methylbulbocapnine and dicentrine suppress LPS-induced inflammatory response by blocking NF-κB and AP-1 activation through inhibiting MAPKs and Akt signaling in RAW264. 7 macrophages. Biol Pharm Bull 41:1219–1227. https://doi.org/10.1248/bpb.b18-00037

Yu L, Han S, Lang L et al (2021) Oxocrebanine: A novel dual topoisomerase inhibitor, suppressed the proliferation of breast cancer cells MCF-7 by inducing DNA damage and mitotic arrest. Phytomedicine 84:153504. https://doi.org/10.1016/j.phymed.2021.153504

Zhao F, Guo Z, Hou F, Fan W, Wu B, Qian Z (2021) Magnoflorine alleviates "M1" polarized macrophage-induced intervertebral disc degeneration through repressing the HMGB1/Myd88/NF-κB pathway and NLRP3 inflammasome. Front Pharmacol 1892. https://doi.org/10.3389/fphar.2021.701087

Zhou D, Huang C, Lin Z et al (2014) Macrophage polarization and function with emphasis on the evolving roles of coordinated regulation of cellular signaling pathways. Cell Signal 26:192–197. https://doi.org/10.1016/j.cellsig.2013.11.004